# Systematic analysis of gut microbiome reveals the role of bacterial folate and homocysteine metabolism in Parkinson's disease

Dorines Rosario, Gholamreza Bidkhori, Sunjae Lee, Janis Bedarf, Falk Hildebrand, Emmanuelle Le Chatelier, Mathias Uhlen, Stanislav Dusko Ehrlich, Gordon Proctor, Ullrich Wüllner, et al.

▶ **To cite this version:**

Dorines Rosario, Gholamreza Bidkhori, Sunjae Lee, Janis Bedarf, Falk Hildebrand, et al.. Systematic analysis of gut microbiome reveals the role of bacterial folate and homocysteine metabolism in Parkinson's disease. Cell Reports, 2021, 34 (9), pp.108807. 10.1016/j.celrep.2021.108807 . hal-03978017

**HAL Id: hal-03978017**
**https://hal.inrae.fr/hal-03978017**

Submitted on 1 Mar 2023

**HAL** is a multi-disciplinary open access archive for the deposit and dissemination of scientific research documents, whether they are published or not. The documents may come from teaching and research institutions in France or abroad, or from public or private research centers.

L'archive ouverte pluridisciplinaire **HAL**, est destinée au dépôt et à la diffusion de documents scientifiques de niveau recherche, publiés ou non, émanant des établissements d'enseignement et de recherche français ou étrangers, des laboratoires publics ou privés.

Distributed under a Creative Commons Attribution 4.0 International License

Cell Reports

Article

# Systematic analysis of gut microbiome reveals the role of bacterial folate and homocysteine metabolism in Parkinson's disease

## Graphical Abstract

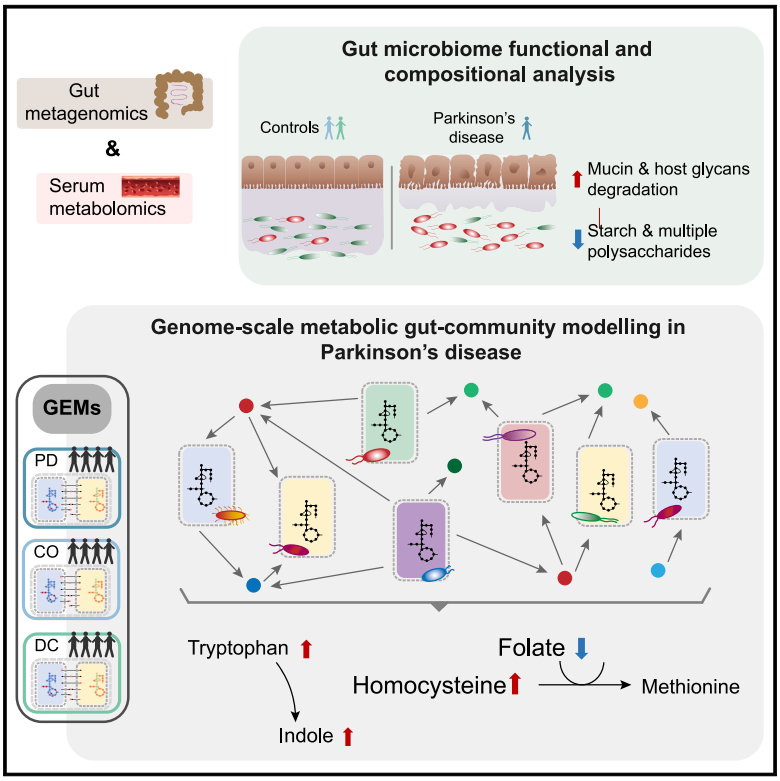


## Authors

Dorines Rosario, Gholamreza Bidkhori, Sunjae Lee, ..., Ullrich Wüllner, Adil Mardinoglu, Saeed Shoaie

## Correspondence

adilm@scilifelab.se (A.M.), saeed.shoaie@kcl.ac.uk (S.S.)

## In brief

Rosario et al. reveal the role of gut microbiome in Parkinson's disease (PD) through functional and compositional analysis and genome-scale metabolic modeling. Microbial capability of mucin and host glycans degradation is associated with disease severity. Gut-community metabolic modeling reveals the bacterial contribution to folic acid deficit and hyperhomocysteinemia in PD.

## Highlights

- Microbiome functional analysis reveals changes in carbohydrate-active enzymes in PD
- Higher number of bacterial mucin and host degradation enzymes link to PD
- Metabolic modeling reveals the contribution of bacterial-specific metabolism in PD
- Gut-community modeling reveals the role of bacterial folate and homocysteine in PD

Rosario et al., 2021, Cell Reports *34*, 108807
March 2, 2021 © 2021 The Authors.
https://doi.org/10.1016/j.celrep.2021.108807

CellPress

Cell Reports

CellPress
OPEN ACCESS

Article

# Systematic analysis of gut microbiome reveals the role of bacterial folate and homocysteine metabolism in Parkinson's disease

Dorines Rosario,[1] Gholamreza Bidkhori,[1] Sunjae Lee,[1,9] Janis Bedarf,[2,3] Falk Hildebrand,[3,4,5] Emmanuelle Le Chatelier,[6] Mathias Uhlen,[7] Stanislav Dusko Ehrlich,[6] Gordon Proctor,[1] Ullrich Wüllner,[2,8] Adil Mardinoglu,[1,7,*] and Saeed Shoaie[1,7,10,*]

[1]Centre for Host–Microbiome Interactions, Faculty of Dentistry, Oral & Craniofacial Sciences, King's College London, SE1 9RT London, UK
[2]Department of Neurology, University Hospital Bonn, Venusberg Campus 1, 53127 Bonn, Germany
[3]Gut Microbes & Health, Quadram Institute Bioscience, Norwich Research Park, Norwich, Norfolk NR4 7UA, UK
[4]European Molecular Biology Laboratory, Structural and Computational Biology Unit, 69117 Heidelberg, Germany
[5]Digital Biology, Earlham Institute, Norwich, Norwich Research Park, Norwich NR4 7UZ, Norfolk, UK
[6]Université Paris-Saclay, INRAE, MGP, 78350 Jouy en Josas, France
[7]Science for Life Laboratory (SciLifeLab), KTH - Royal Institute of Technology, Tomtebodavägen 23, 171 65 Solna, Stockholm, Sweden
[8]German Centre for Neurodegenerative Disease Research (DZNE), 53127 Bonn, Germany
[9]Present address: School of Life Sciences, Gwangju Institute of Science and Technology, Gwangju, Republic of Korea, 61005
[10]Lead contact
*Correspondence: adilm@scilifelab.se (A.M.), saeed.shoaie@kcl.ac.uk (S.S.)
https://doi.org/10.1016/j.celrep.2021.108807

## SUMMARY

Parkinson's disease (PD) is the most common progressive neurological disorder compromising motor functions. However, nonmotor symptoms, such as gastrointestinal (GI) dysfunction, precede those affecting movement. Evidence of an early involvement of the GI tract and enteric nervous system highlights the need for better understanding of the role of gut microbiota in GI complications in PD. Here, we investigate the gut microbiome of patients with PD using metagenomics and serum metabolomics. We integrate these data using metabolic modeling and construct an integrative correlation network giving insight into key microbial species linked with disease severity, GI dysfunction, and age of patients with PD. Functional analysis reveals an increased microbial capability to degrade mucin and host glycans in PD. Personalized community-level metabolic modeling reveals the microbial contribution to folate deficiency and hyperhomocysteinemia observed in patients with PD. The metabolic modeling approach could be applied to uncover gut microbial metabolic contributions to PD pathophysiology.

## INTRODUCTION

Parkinson's disease (PD), a progressive neurological disorder with a presumed multifactorial etiology (Chin and Vora, 2014; Ma, 2018), is the most common neurodegenerative disease compromising motor functions (Brown et al., 2005; Gammon, 2014). Nonmotor symptoms (NMSs) commonly cause morbidity in later stages of PD (Aarsland et al., 2017). PD is a heterogeneous multi-systemic disorder (Aarsland et al., 2017; Lee and Koh, 2015), and its pathophysiology is only partially understood (Antony et al., 2013). A growing body of evidence links the gastrointestinal (GI) tract to PD, opening possibilities for diagnosis and treatment (Braak et al., 2006; Fasano et al., 2015; Pfeiffer, 2011; Savica et al., 2009). GI dysfunction is a common NMS experienced by people with PD (Fasano et al., 2015; Pfeiffer, 2011). Hence, it is necessary to elucidate the underlying molecular mechanisms of the gut in the development and progression of PD for a better understanding of the bidirectional interactions within the gut-brain axis. Analysis of the microbiota of sigmoid mucosal biopsies and stool samples from patients with PD revealed significant alterations in the composition of the gut microbiota (Keshavarzian et al., 2015; Scheperjans et al., 2015), with a significant decrease in the abundance of bacteria with anti-inflammatory features and a significant increase in the abundance of pro-inflammatory species (Keshavarzian et al., 2015). It has been reported that the abundance of the genes involved in lipopolysaccharide (LPS) biosynthesis and type III bacterial secretion systems is increased in people with PD (Keshavarzian et al., 2015). Furthermore, the abundance of *Enterobacteriaceae* is positively correlated with motor impairment, suggesting that dysbiosis in the microbiome of patients with PD is related to the disease-motor phenotype (Scheperjans et al., 2015). In addition to GI and motor dysfunction, gut microbial metabolic changes could trigger neuroinflammation in a model of PD (Sampson et al., 2016). Microbial alterations and inflammatory cascades underlying gut leakiness facilitate the translocation of pathogens and toxic bacterial fragments capable of reaching the central nervous system (CNS). Subsequently, a mouse


This is an open access article under the CC BY license (http://creativecommons.org/licenses/by/4.0/).

model of PD has shown that the inflammation of the mucosal layer and the associated state of oxidative stress can initiate alpha-synuclein-aggregate (α-syn) accumulation in the enteric nervous system (ENS) (Kim et al., 2019).

PD has been studied from the perspective of the gut-brain axis (Chiang and Lin, 2019; Gerhardt and Mohajeri, 2018). However, the metabolic interactions between gut bacteria and their contribution to disease progression have not been fully investigated. To elucidate these interactions, individual- and systems-level analysis is required. Therefore, systems biology approaches could be applied to reveal associations between the abundances of different microbes and the molecular mechanisms underlying PD on a functional level (Witherden et al., 2017; Mardinoglu et al., 2018; Rosario et al., 2020). Genome-scale metabolic models (GEMs) have been applied to gain detailed understanding of microbial metabolic changes in different environments (Gu et al., 2019). GEMs have been previously employed to reveal the metabolic interactions among bacteria as well as between the bacteria and the host (Mardinoglu et al., 2015; Rosario et al., 2018; Shoaie et al., 2013; Tramontano et al., 2018). Therefore, efforts have been made to develop methods capable of metabolic modeling of microbial community and apply this in the gut microbiome (Baldini et al., 2019; Shoaie et al., 2015).

Bedarf et al. (2017) collected fecal samples from people with PD and generated metagenomics data for analyzing the species abundances. The cohort comprised 31 early-stage L-DOPA-naive PD male individuals and 28 matched controls. In the present study, the metagenomics data from this cohort have been re-analyzed with improved metagenome species profiles. We applied an integrative correlation network (ICN) approach, which provides insight into the common and unique microbial species associated with PD severity, GI dysfunction, and age. We analyzed the carbohydrate-active enzymes (CAZymes) of the significantly altered species and found that the abundance of the genes associated with degradation of mucin and host glycans was increased in patients with PD and linked with disease severity, GI dysfunction, and age in people with PD. We performed personalized community-level modeling using the GEMs, and our analysis revealed a decreased production of folate and an increased production of homocysteine in patients with PD. We generated targeted metabolomics data using the serum samples collected from patients with PD of the same cohort. Metabolomics and metagenomics data were integrated using GEMs to study the effect of the microbiome on the host metabolism. The integrative metabolic modeling approach enabled the identification of the roles played by gut microbiota in the host metabolism contributing to PD pathophysiology.

## RESULTS

### Profiling the gut microbial compositional changes in the PD cohort

We quantified publicly available shotgun metagenomics data of 31 male patients with early-stage levodopa (L-DOPA)-naive PD and 28 matched controls (Bedarf et al., 2017). In the metagenomics data analysis, we used the latest available human gut microbiome catalog (Wen et al., 2017) to determine the gene abundances (Method details). Using metagenome species pangenomes (MSPs), our analysis facilitated the identification of perturbed gut microbial species with more in-depth functional annotations of the key metagenome species. Because of data processing requirements to keep deep-sequenced samples (see Method details), we removed a few samples and re-analyzed the metagenomics data of 26 PD and 25 controls, of which 11 were healthy controls (COs) while 14 were diseased controls (DCs) with cardiovascular risk factors. For simplicity, we refer in the text to both the COs and DCs, unless otherwise specified. Here, the microbiome compositional change between PD and control was defined as PD dysbiosis. The significant taxonomic changes at the phylum, family, and genus levels between patients with PD and controls can be found in Table S1 and Figure S1. We performed enterotype analysis by unsupervised clustering and found three clusters enriched with *Bacteroides*, Firmicutes, and *Prevotella* enterotypes (Method details). We observed that the microbiome of patients with PD was clustered into *Bacteroides* and Firmicutes enterotypes and was related to richness (Figure 1A). Unlike in the controls among PD samples, there was no *Prevotella* enterotype.

The species-level abundances (Wilcoxon signed-rank test, false discovery rate [FDR] < 0.05) of 132 MSPs were significantly altered between people with PD and controls: 73 MSPs were significantly increased (16 classified at all taxonomic levels), while 59 MSPs were significantly decreased (32 of classified at all phylogenetic levels) in PD (Table S1). We also identified significant changes specific to each subgroup of the controls. The abundances of 3 and 19 classified MSPs were significantly increased and decreased between PD and COs, respectively. Comparing PD to DCs, the abundances of 11 classified MSPs were significantly increased, while 26 classified MSPs were significantly decreased, of which 5 are *Prevotella* spp., 6 are *Lactobacillus* spp., and 3 are *Streptococcus* spp. The use of the MSPs and gut microbial gene catalog enabled the identification of additional species with altered abundance in patients with PD compared to controls (Figure 1B). In accordance with the original study (Bedarf et al., 2017), the abundances of *Akkermansia muciniphila* and *Alistipes shahii* were significantly increased, while the abundances of *Prevotella copri* and *Clostridium saccharolyticum* were significantly decreased in PD compared to controls. We identified additional species— *Alistipes obesi*, *Alistipes ihumii*, and *Candidatus gastranaerophilales*—with significantly higher abundances in patients with PD than in controls. *Ruthenibacterium lactatiformans* was significantly increased in people with PD compared to COs, while *Clostridium spiroforme* was significantly increased in PD compared to disease controls. *Methanobrevibacter smithii_2* (*M. smithii_2*), a major human gut archaea producer of methane (Gaci et al., 2014; Triantafyllou et al., 2014), was significantly increased in PD. *Desulfibrio piger*, a sulfate reducer, was significantly decreased in PD compared to controls, and *Roseburia intestinalis* and *Faecalibacterium prausnitzii*, both butyrate producers (Horz and Conrads, 2010), were decreased compared to COs. Another strain of *F. prausnitzii* and a second strain of *P. copri* were significantly depleted in patients with PD compared to DCs.

CellPress
OPEN ACCESS

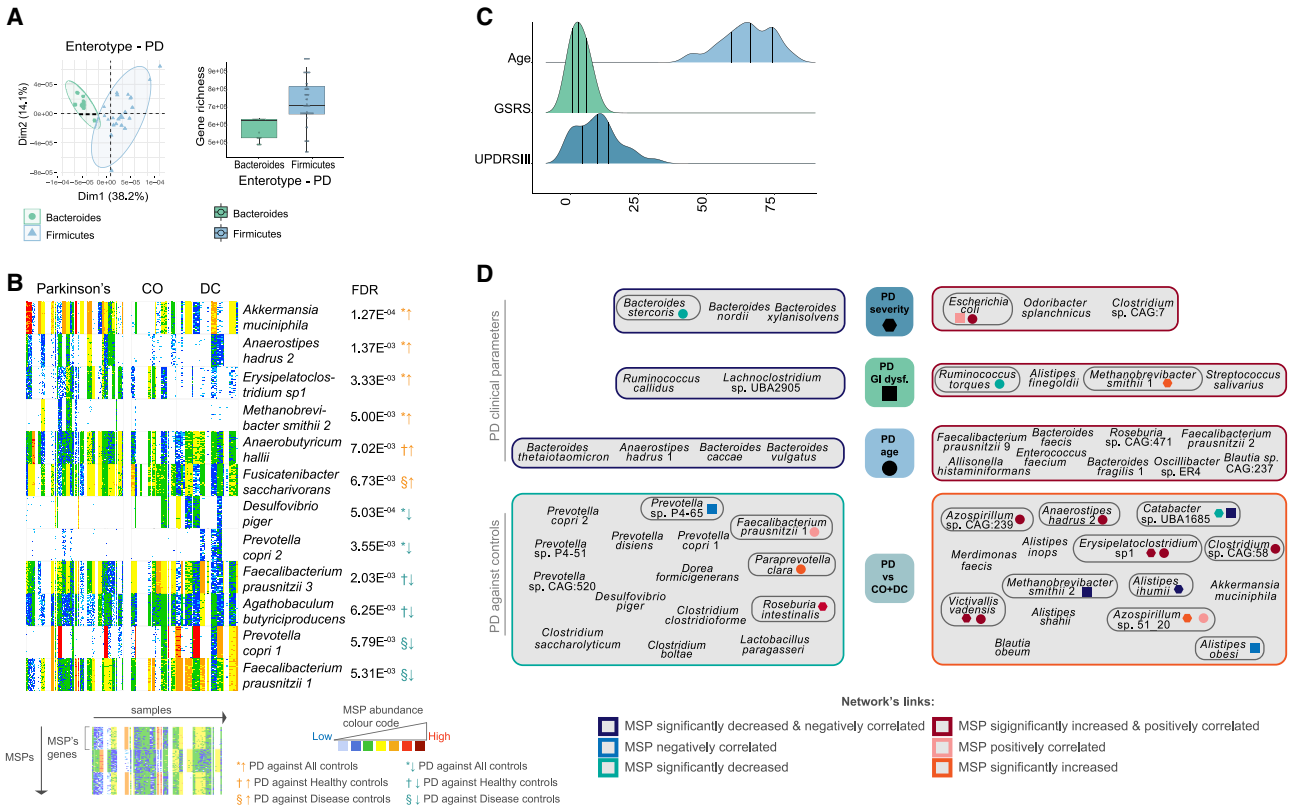


**Figure 1. Enterotype and microbial compositional changes**

(A) Left: enterotype for PD samples. Principle component analysis (PCA) plot represents PD samples highlighted by enterotype. Right: relation between gene richness and enterotype of PD samples.

(B) Barcodes of significantly increased and decreased (Wilcoxon signed-rank test, FDR < 0.05) MSPs between PD and controls (asterisks), PD and healthy controls (COs) (crosses), and PD and diseased controls (DCs) (silcrows). Barcodes represent each sample in the group and respective gene counts of each gene clustered into MSPs. Sample size under analysis: 26 samples of PD and 25 controls, of which 11 were COs and 14 were DCs with cardiovascular risk factors.

(C) Distribution and quartiles illustration of age, GSRS scores representative of GI function, and UPDRS III scores used to gauge disease progression and severity. Sample size of first and fourth quartiles of PD clinical parameters: PD severity 8 and 6 samples, respectively; PD GI dysfunction contains 7 samples in each quartile; PD age with 7 and 8 samples, correspondingly.

(D) Integrative correlation network (ICN) based on MSPs significance and Spearmen correlation between PD and controls and metadata of patients with PD (Wilcoxon signed-rank test, FDR < 0.05). PD dysbiosis represents MSPs with abundance significantly increased or decreased between PD and controls. The network of PD-related clinical parameters shows MSPs that were both correlated and significantly altered with respect to age of patients with PD, disease severity, and GI dysfunction. In the network, species circled in gray were found to be associated with more than one clinical parameter in PD and/or dysbiosis against controls. Squared, circled, and hexagonal shapes are related to GI dysfunction, age, and disease severity, respectively. The coloring of these shapes in circled species represents the microbe association with additional clinical parameters.

## The gut microbiome compositional changes were associated with disease severity, GI dysfunction, and age in patients with PD

Besides PD dysbiosis, we determined taxonomic alterations considering clinical parameters of patients with PD. The Unified PD Rating Scale III (UPDRS) score was used to gauge the course of PD in the cohort, here referred as PD severity. A modified version of the GI Symptom Rating Scale (GSRS; see original study [Bedarf et al., 2017]) score was applied to infer GI symptoms in people with PD, referred to as GI dysfunction. Spearman's correlation was used to determine the associations between the abundances of gut microbiota and PD severity, GI dysfunction, and the age of patients with PD (Wilcoxon signed-rank test, FDR < 0.05). To identify significant alterations in bacterial abundances considering each clinical parameter in PD, we clustered patients into quartiles based on individual metadata information (Figure 1C) and identified the differences between the microbial abundances of the first and fourth quartiles using the Wilcoxon signed-rank test (FDR < 0.05). Detailed analysis on MSPs with significantly altered abundance associated with PD clinical parameters and/or correlated MSPs abundances are laid out in Table S2 and Figure S2.

Based on these results and classified MSPs associated with PD and clinical data, we constructed an ICN to better understand the interactions between the species and their relevance to different clinical data (Figure 1D; Method details). ICN results revealed that the abundance of *Escherichia coli* (*E. coli*) is significantly increased and positively correlated with age, PD severity, and increased GI dysfunction in patients with PD. *Erysipelatoclostridium* sp1 and *Victivallis vadensis* were significantly

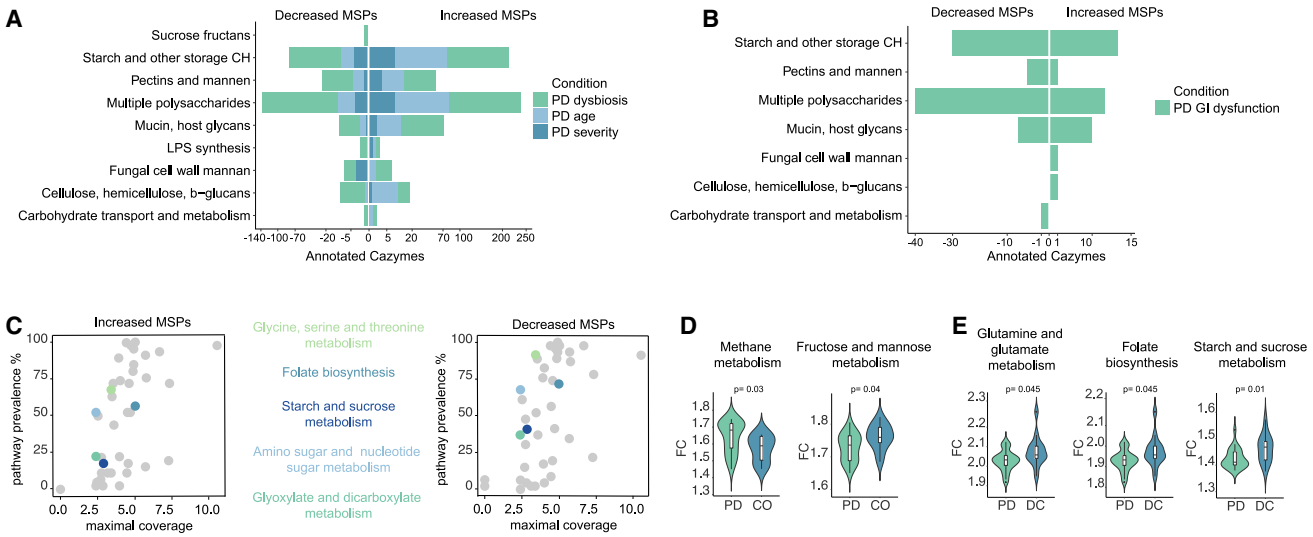


**Figure 2. Functional annotation of the altered MSPs**

(A and B) Carbohydrate-active enzymes (CAZymes) genes annotation of significantly increased and decreased (Wilcoxon signed-rank test, FDR < 0.05) MSPs in PD dysbiosis (PD against controls), PD severity (UPDRS III score), PD GI dysfunction (GSRS), and PD patients' ages. Genes annotated to mucin and host glycans degrading CAZymes were higher in MSPs significantly increased in PD compared to controls, disease severity, GI dysfunction, and age of people with PD.

(C) Metabolic pathway prevalence and maximal coverage of significantly (Wilcoxon signed-rank test, FDR < 0.05) increased and decreased MSPs (PD compared to controls), where maximal coverage represents the highest pathway coverage in each set of MSPs (significantly increased and decreased).

(D and E) Significant personalized metabolic pathways enrichment based on GEMs for MSPs in PD (26 samples) compared to COs (11 samples) (Wilcoxon signed-rank test, $p < 0.05$) (D) and in PD compared to DCs (14 samples) (E).

increased in PD compared to controls and positively correlated with diseased severity and age of people with PD. Another strain of *Erysipelatoclostridium* sp. was increased in PD compared to DCs and increased with greater GI dysfunction in patients with PD (Figure S1). Abundances of *Azospirillum* sp. 51_20 and *Azospirillum* sp. CAG:239 were significantly increased in PD compared to controls and were positively correlated with age. As previously mentioned, the abundance of *M. smithii*_2 was significantly increased in PD compared to controls, while ICN analysis showed *Methanobrevibacter smithii*_1 was significantly increased and positively correlated with GI dysfunction and significantly increased with disease severity.

## Mucin and host glycan degradation was associated with PD dysbiosis, severity, GI dysfunction, and age

As carbohydrate metabolism is one of the key features in the gut microbiome, CAZymes analysis on genes was used to identify potential alterations in the microbial conversion of carbohydrates (Table S3). Overall, we found an increased number of annotated mucin and host glycan degradation gene-coding CAZymes in MSPs with increased abundance in PD compared to controls, and MSPs increased in patients with PD with more severe disease, GI dysfunction, and older people with PD (Figures 2A and 2B). The abundance of *A. muciniphila*, which is well known for its capability to degrade host glycans and mucins (Kovatcheva-Datchary et al., 2019), was significantly increased in PD. MSPs with capacity for LPS synthesis was increased in older patients with PD and in more severe disease. We found an increased number of annotated CAZymes associated with the conversion of multiple polysaccharides, pectins, mannan, starch, and other storage carbohydrates in MSPs with significantly increased abundance in PD compared to controls in more severe and elderly individuals with PD. In contrast, people with PD with more severe GI dysfunction showed an increased number of these annotated CAZymes in MSPs with significantly decreased abundance.

## GEMs for pathway analysis of associated MSPs with PD

To gain a mechanistic understanding of gut microbiota metabolism in PD and reveal the interactions between the gut microbes and their contribution to host metabolism, we generated GEMs for the selected 158 MSPs with significantly changed abundances compared to controls and significantly altered depending on disease severity, GI dysfunction, and age (Figure S3). We used these metabolic models for personalized community-level metabolic modeling and in-depth pathway analysis (Method details). A matrix of reaction abundance was generated for each patient and control based on MSP abundances and reactions in the GEMs. We used Kyoto Encyclopedia of Genes and Genomes (KEGG) metabolic pathways to identify the differences between the prevalence of metabolic reactions. Maximal coverage was used, representing the highest pathway coverage in each set of MSPs under each clinical condition (Method details). We analyzed maximal coverage and pathway prevalence in significantly increased and decreased sets of MSPs in people with PD. Enrichment analysis of bacterial metabolic pathways with respect to gut microbial perturbations revealed starch, sucrose, glycine, serine, and threonine metabolisms to be more prevalent in decreased MSPs in PD compared to controls. Prevalence of folate biosynthesis was also higher in MSPs that were decreased in PD compared to controls (Figure 2C). Arginine and

proline metabolisms revealed higher prevalence in MSPs with increased abundances in higher stages of disease severity. Similar trends were observed for valine, leucine, and isoleucine biosynthesis. In contrast, the prevalence of riboflavin metabolism was found to be higher in MSPs decreased in more severe PD (Figure S4). Methane metabolism was more prevalent in increased MSPs in people with PD with increased GI dysfunction. Reduced thiamine metabolism was the main metabolic feature associated with increased GI dysfunction, being more prevalent in MSPs decreased in more severe GI dysfunction (Figure S4). Both riboflavin metabolism and folate biosynthesis were more prevalent in decreased MSPs in older people with PD (Figure S4). Glyoxylate and dicarboxylate metabolism were more prevalent in decreased MSPs related to PD dysbiosis, disease severity, and age but were also more prevalent in augmented MSPs with increased GI dysfunction.

Personalized metabolic pathway enrichment was performed using the reaction abundance matrix. Through KEGG pathway enrichment analysis, we identified significant alterations between PD and controls and between PD and each sub-control group ($p < 0.05$) (Method details). Methane metabolism was significantly increased in PD compared to healthy individuals (Figure 2D). Based on pathway enrichment analysis using functional metabolic models, glutamine and glutamate metabolism were significantly decreased in PD compared to DCs. Bacterial folate biosynthesis was also significantly decreased in PD compared to DCs (Figure 2E). The starch and sucrose metabolic pathways were significantly decreased in PD compared to disease controls, while fructose and mannose metabolism were significantly decreased in PD compared to COs.

### GEM of individual species associated with PD

GEMs for selected MSPs were used for constraint-based modeling. We performed flux balance analysis (FBA) for each GEM to assess the bacterial growth rate and the major metabolic activities of each MSP (Method details). Simulations showed lower bacterial growth rate for significantly increased species under four PD clinical conditions of interest in comparison to depleted species (Figure 3A). Based on GEMs for increased and decreased MSPs identified in PD, we investigated the consumption and production of each metabolite. There was specific microbial metabolic alteration related to each distinct PD condition, such as higher production of indole by increased species (PD compared to controls) (Figure 3B). Moreover, propionate and butyrate production were linked to decreased species in PD dysbiosis and severity (Figure S5). Additionally, the simulations showed that mannose consumption was higher in species decreased in PD dysbiosis and more severe PD. Proline production was higher in species significantly increased with PD severity. Production of glycine and arginine was higher by depleted species in increased stages of GI dysfunction in PD (Figure S5). Moreover, hydrogen sulphide ($H_2S$) production was higher in species with increased abundance in PD dysbiosis and severity. Ammonia ($NH_3$) production was higher in species with increased abundance in PD dysbiosis and people with PD with increased GI dysfunction. Based on FBA predictions, we assessed the potential contribution of bacteria to the gut microbiome metabolism.

### Personalized-level metabolic community modeling and metabolomics revealed the gut microbial contribution to altered metabolism in patients with PD

Metabolic modeling of individual MSPs enabled the assessment of species-level potential role in overall gut microbial metabolism. However, the individual microbial activity is different in a microbial community considering the abundances of species and the availability of nutrients. Thus, for a deeper understanding of the contribution of the gut microbiota to host metabolism in patients with PD, we reconstructed personalized community models for each individual in the PD cohort (25 PD, 10 CO, 13 DC) (Method details). Personalized-level community modeling indicated that the microbial production of homocysteine, glycine, isoleucine, glutamate, nitrate, and valine was significantly increased in patients with PD compared to controls (Figure 3C). Personalized community models also indicated that microbial secretion of cysteine, cysteine-glycine, and taurine was higher in PD. Additionally, we predicted that microbial production of $NH_3$, $H_2S$, and hydrogen peroxide ($H_2O_2$) is increased in PD communities (Figure 3D). Moreover, the secretion of tryptophan, indole, ornithine, phenylalanine, and putrescine was predicted to be increased in PD compared to controls. On the other hand, the production of folate, glutamine, carnosine, and succinate is predicted to be decreased in patients with PD.

To evaluate the predictions, we generated targeted metabolomics data using the serum samples obtained from 8 PD, 5 CO, and 5 DC subjects of the same PD cohort (Table S4). Based on analyte class, there were increased levels of indoles and derivatives in PD compared to controls (Figure 4A). Similarly, sphingomyelins and biogenic amines were increased, whereas the profile of bile acids and fatty acids was decreased in PD compared to controls. Partial least-squares-discriminant analysis (PLS-DA) between PD and controls was performed using the metabolomics data and identified significantly different metabolites ($p < 0.05$) (Table S5). Hippuric acid and indolepropionic acid (IPA), previously associated with gut microbiota (Wikoff et al., 2009), were significantly increased in PD compared to COs and DCs (Figure 4B). Tryptophan betaine was significantly increased, while indoxyl sulfate was significantly decreased in PD compared to COs.

Personalized gut-microbiota community modeling and plasma metabolomics were integrated for a holistic understanding of gut microbiome-host metabolic interactions. Based on the modeling of the gut microbial community, we were able to identify those species within the community that may contribute to the production/consumption of metabolites. There was an increased microbial production of indole and tryptophan in PD compared to controls. *A. muciniphila*, *A. ihumii*, *A. shahii*, and *C. gastranaerophilales* were found to be the main producers of indole, while *A. muciniphila*, *Erysipelatoclostridium* spp., and a species of *Eubacterium* contributed to tryptophan secretion (Figure 5). Metabolomic profiling of serum samples showed increased concentrations of indoles and derivatives in PD samples compared to controls. IPA concentration was significantly increased in PD, while the concentration of indoxyl sulfate was significantly decreased. Moreover, levels of folate were decreased in PD compared to controls, and increased secretion of homocysteine was verified in PD communities.

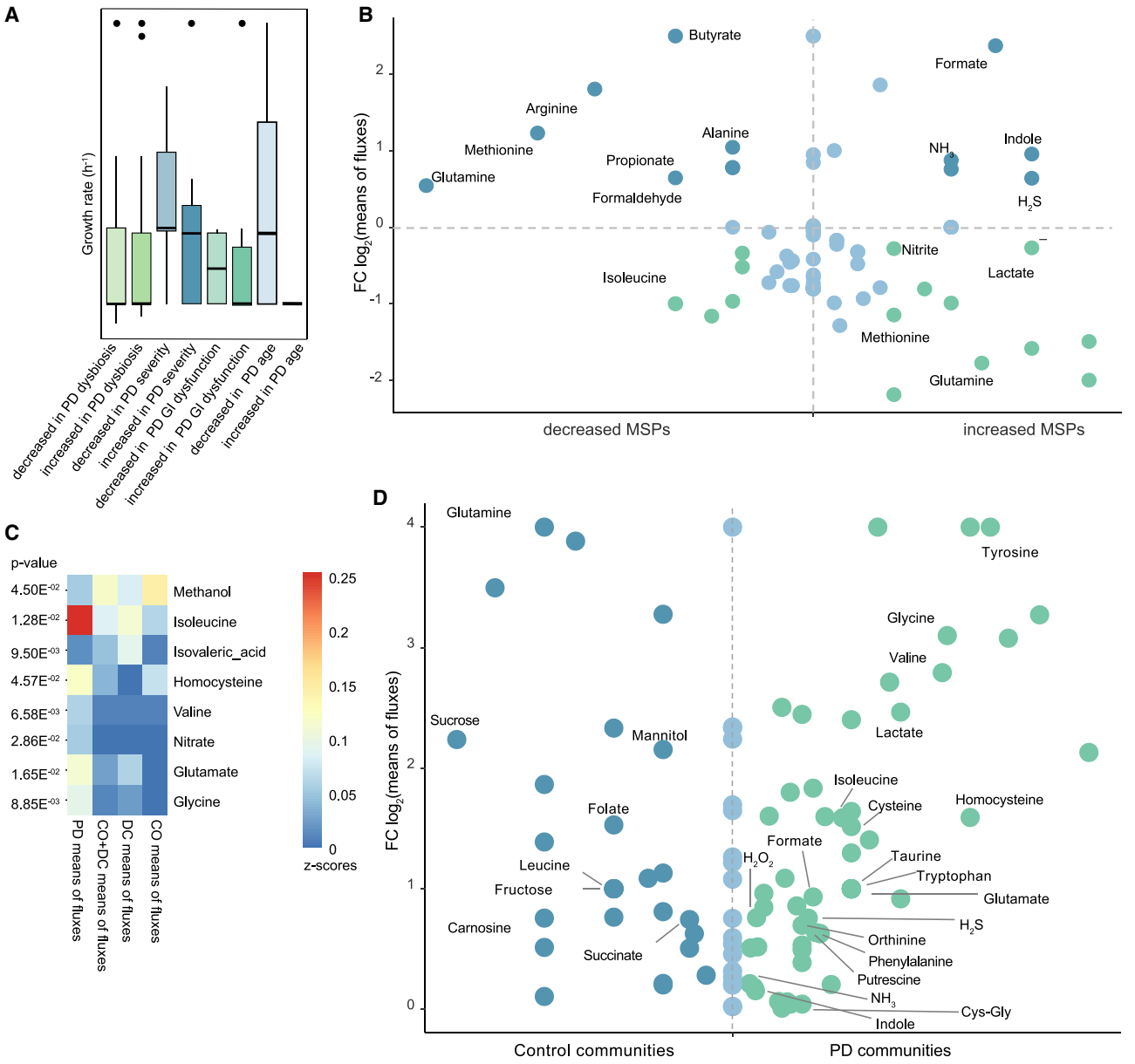


**Figure 3. GEM of individual MSPs and personalized gut microbial community modeling of the PD cohort**

(A) Predictions of individual bacterial growth rate ($h^{-1}$). Overall, MSPs with significantly decreased abundance revealed a higher growth rate in comparison to MSPs with significantly increased abundance.

(B) Potential contribution to host-intestinal metabolic pool based on metabolites production and consumption of significantly increased and decreased MSPs in PD dysbiosis (Wilcoxon signed-rank test, FDR < 0.05). The x axis represents the number of decreased or increased MSPs contributing to the metabolite consumption or production in y axis (green negative or blue positive values, respectively).

(C) Personalized gut microbial community modeling of each subject from the PD metagenomics cohort: 25 PD communities and 23 control communities, from which 10 were COs and 13 were DCs. Significantly (Wilcoxon signed-rank test, $p < 0.05$) different fluxes (FBA-based predictions) of secreted microbial metabolites are shown between gut-community models of patients with PD and controls. The heatmap shows the *Z* scores of the means of microbial-metabolites fluxes in each group.

(D) Potential contribution of gut microbiota to host intestinal metabolic pool, based on personalized gut microbial community modeling FBA predictions. Blue, increased secretion of microbial metabolites in controls communities compared to PD; green, increased secretion of microbial metabolites in PD communities compared to controls.

Based on the community modeling, we identified *Paraprevotella clara*, *Prevotella* sp., and *R. intestinalis* were decreased in PD compared to controls and produced folate. *A. muciniphila*, *Subdoligranulum* sp., *Eubacterium* sp., and Clostridiales family XIII were identified as the main producers of homocysteine and increased in PD compared to controls. We performed

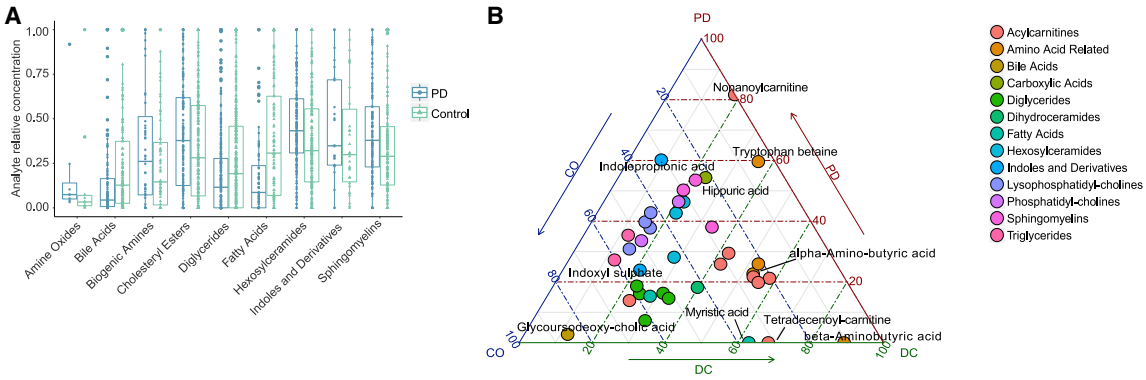


**Figure 4. Metabolomics of serum samples from 8 patients with PD, 5 COs, and 5 DCs**

(A) Relative concentration of analytes class in PD and controls.

(B) Significant metabolites between PD and both controls, PD and COs, and PD and DCs (Wilcoxon signed-rank test, $p < 0.05$). Metabolite position in the barycentric diagram depicts the concentration ratios of the metabolite across the three groups. These metabolites were also found as features of the principal components of partial least-squares-discriminant analysis (PLS-DA) between PD and controls.

Spearman's correlation analysis between the fluxes predicted by the community models, from which we have identified the microbial producers within the communities and the MSPs abundances in the metagenomics samples. We have found that metabolite levels significantly correlated with abundances of relevant bacteria (Table S6).

## DISCUSSION

Downstream analysis of gut microbial abundance alterations between PD and controls using the latest improved human gut microbiome catalog allowed an extended identification of perturbed gut microbial species and strains in PD (Wen et al., 2017). We generated GEMs for key species and performed pathway analysis and individual- and community-level modeling with integration of serum metabolomics data. These analyses provided insights into the metabolic contribution of gut microbiota to PD pathophysiology.

We observed a decrease in the abundances of bacterial short-chain fatty acids (SCFAs)-producing bacteria. *B. thetaiotaomicron* has protective effects due to the anti-inflammatory activity of its pirin-like protein, reducing proinflammatory nuclear factor κB (NF-κB) signaling in epithelial cells (Delday et al., 2019). The absence of *Prevotella* was observed in PD, and this could be linked to gut microbiome dysfunction in people with PD and consequently contribute to the alterations in the ENS (Borre et al., 2014). Depletion of *Prevotellaceae* has also been reported previously in patients with PD (Keshavarzian et al., 2015). Increase of *A. muciniphila* abundance and decrease of *Prevotella* could be inferred as higher mucus degradation that may result in gut permeability in people with PD (Forsyth et al., 2011). This was also observed in CAZymes analysis, which indicated increased mucin and host glycan degradation, decreased polysaccharide degradation, and increased LPS synthesis in elderly patients with PD and higher severity of PD. Increased gut permeability facilitates the translocation of pro-inflammatory bacterial products such as LPS. Bacterial fragments like LPS promote pro-inflammatory stimuli that trigger α-syn aggregation and deposition in the ENS and might thus contribute to the development and pathogenesis of PD (Braak et al., 2006; Keshavarzian et al., 2015).

In our study, the abundance of *E. coli* was significantly increased and positively correlated with disease severity and age in people with PD. Additionally, it was found to be positively correlated with GI dysfunction in PD. Previous research has shown that increased intestinal biopsy staining for α-syn and nitrotyrosine, indicative of oxidative stress in the sigmoid mucosa with stained *E. coli*, is linked with intestinal hyperpermeability in PD (Forsyth et al., 2011). Translocation of endotoxins into the colonic mucosa can trigger a pro-inflammatory cascade of events and might be involved in the progression of neuroinflammation in the ENS and CNS in patients with PD (Forsyth et al., 2011). *E. coli* is known for its inflammatory activity, and its abundance is positively correlated with proinflammatory cytokines interleukin (IL)-1b, NLRP3, and CXCL2 of the peripheral inflammatory state in cognitively impaired elderly patients (Cattaneo et al., 2017). In addition to its role in triggering intestinal inflammation, *E. coli* has amyloidogenic properties by contributing extracellular bacterial amyloid protein curli (Chen et al., 2016). Besides the ~30 amyloidogenic proteins encoded by the human genome, the intestinal microbiota also produces functional amyloids such as curli, which are amyloid proteins abundantly expressed by certain gut bacteria (Sampson et al., 2020). Aged rats exposed to bacterial producers of amyloid protein curli, including *E. coli*, have demonstrated increased deposition of misfolded α-syn in both gut and brain (Chen et al., 2016). Curli protein produced by *E. coli* promoted α-syn pathology in the gut and brain of mice overexpressing human α-syn (Sampson et al., 2020). Such evidence suggests that exposure to bacterial amyloid in the GI tract, from an increased abundance of *E. coli*, might trigger or accelerate α-syn aggregation in the gut and brain, therefore contributing to PD pathogenesis (Chen et al., 2016; Sampson et al., 2020).

Increased abundance of *M. smithii* could have a negative impact on fecal butyrate concentrations (Horz and Conrads, 2010; Triantafyllou et al., 2014) since methanogens live in

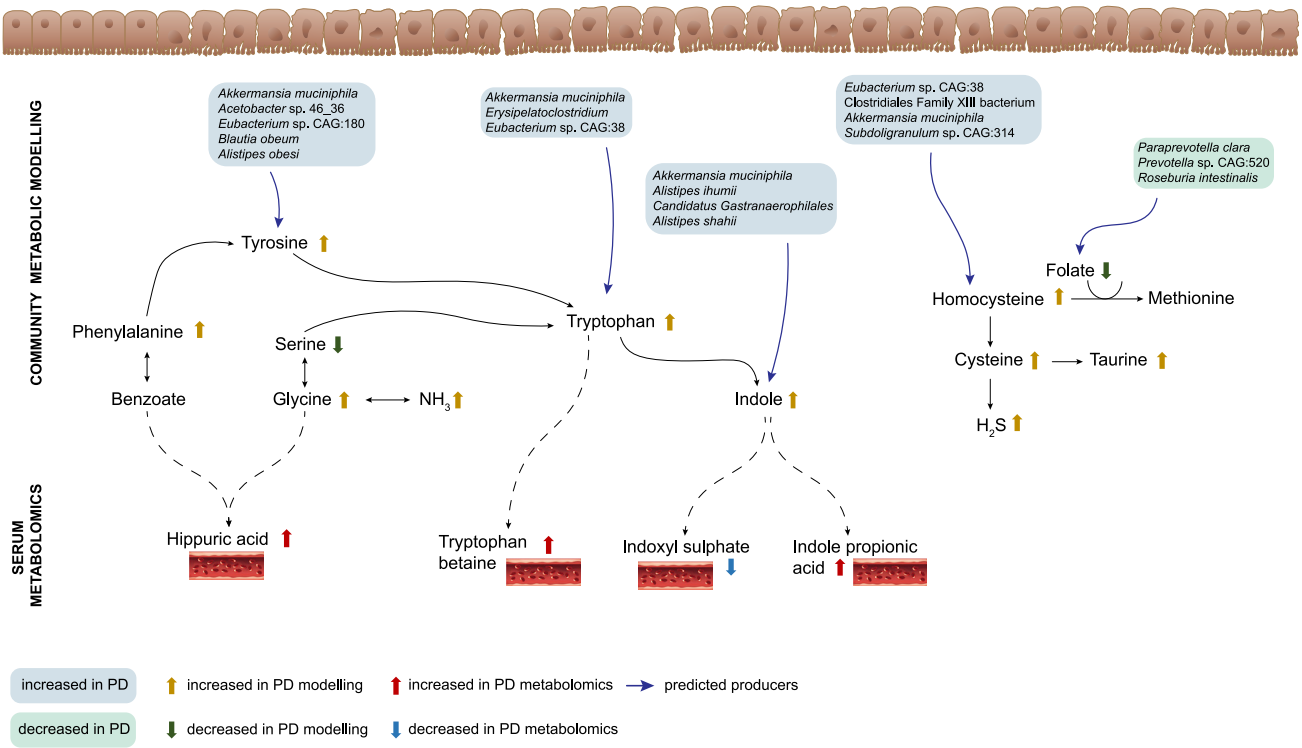


**Figure 5. Personalized gut-microbial community predictions and links to the serum metabolomics of patients with PD**

Top: predictions of metabolic modeling of personalized gut-microbiota communities (PD versus controls). Increased microbial-metabolites secretion (yellow arrow) in PD and decreased microbial metabolites production (green arrow) in PD. FBA predictions of main microbial producers are indicated for metabolites of interest (purple arrow). Bottom: significantly increased (red arrow) and decreased (blue arrow) metabolites in serum samples of patients with PD compared to controls.

syntrophy with butyrate-degrading bacteria. Moreover, methanogens outcompete acetogens and reduce the bioavailability of acetate (Horz and Conrads, 2010). Thus, *F. prausnitzii* and *R. intestinalis*, both known to produce butyrate from acetate (Horz and Conrads, 2010), could be outcompeted by an increased *M. smithii* abundance in patients with PD. Methane, produced by methanogens, has been linked to chronic constipation (Triantafyllou et al., 2014), one of the most commonly reported NMSs in patients with PD (Fasano et al., 2015; Pfeiffer, 2011; Savica et al., 2009). The neuromuscular transmitter role of methane has been suggested to propagate the peristaltic movement of the intestine (Triantafyllou et al., 2014). The gut microbial perturbations identified demonstrated a shift toward a proinflammatory state with the stimulus of an oxidative state and the depletion of gut-microbial anti-inflammatory activity. Such pathophysiologic alterations have been suggested as triggers of $\alpha$-syn aggregation and deposition in the ENS in PD (Chiang and Lin, 2019; Scheperjans et al., 2015).

We also showed that thiamine metabolism decreased in higher stages of GI dysfunction in people with PD. The prevalence of folate biosynthesis and riboflavin metabolism was decreased in elderly individuals with PD. Personalized pathway enrichment analysis demonstrated that folate biosynthesis was significantly decreased in PD. Folate biosynthesis in gut could also impact the homocysteine level. Our modeling showed increase microbial production of homocysteine in the gut communities of patients with PD. A previous study has also reported decreased vitamin levels of thiamine and folate in individuals with PD (dos Santos et al., 2009). A low-folic-acid diet administered to a mouse model resulted in the development of motor symptoms identical to PD, accompanied by increased levels of homocysteine, which demonstrated that folate indirectly impacts dopaminergic neurofunction and dopaminergic neuron cells' death (Duan et al., 2002). In accordance, there is previous evidence of folic acid deficiency as a major determinant of hyperhomocysteinemia in PD (dos Santos et al., 2009), possibly because the breakdown of homocysteine can be through its remethylation, converted to methionine in a reaction dependent on folate metabolism and vitamin $B_{12}$. Alternatively, the pathway for homocysteine metabolism can be through transsulfuration via cysteine (Müller, 2008). Hyperhomocysteinemia is considered a risk factor for the development of atherosclerosis (Guthikonda and Haynes, 2006), cognitive disorders, and neuropathies (Xie et al., 2017). Moderately increased homocysteine plasmatic levels have also been linked to endothelial dysfunction (Chambers et al., 1998). A previous study interested in understanding the effects of acute L-DOPA intake on homocysteine levels in patients with PD revealed that L-DOPA metabolism (measured by the drug absorption after intake) is an important component contributing to homocysteine levels (Müller and Kuhn, 2009). Chronic (Müller, 2008) L-DOPA intake increased

the plasma levels of homocysteine, following O-methylation of L-DOPA to 3-O-methyldopa with production of homocysteine via the methyl-group donor of methionine/S-adenosylmethionine. Increased levels of homocysteine might aggravate PD progression (Müller, 2008). Therefore, vitamin supplementation (e.g., folic acid) has been suggested to complement L-DOPA therapy (Chen et al., 2004). However, the patients in our study were L-DOPA naive.

In addition, gut-community modeling showed increased levels of indole and tryptophan in PD. We predicted that *A. muciniphila*, *A. ihumii*, *A. shahii*, and *C. gastranaerophilales*, whose abundance was significantly increased in PD, contribute to increased concentrations of indole, which could be converted into IPA. Metabolomics analysis of serum revealed that IPA was significantly increased in people with PD. IPA is known for its anti-inflammatory properties in the GI tract and periphery (Tuomainen et al., 2018; Wlodarska et al., 2017; Zhao et al., 2019). Our results showing increased IPA differ with the functional implications of the GI tract in the pathophysiology of PD that move toward a pro-inflammatory environment. Further studies are required to understand this divergence in findings. Intestinal microbiota may evolve to compensate the disruption in gut homeostasis and limit the inflammation, which could be revealed by a longitudinal study of the gut microbiome in PD. It is also important to untangle drug interactions with the microbiome, given that PD medications such as metformin are suggested to affect the gut microbiome (Rosario et al., 2018; Wu et al., 2017). Complementary, future studies considering the dietary routine of patients with PD are of interest, as adaptation of the diet could improve GI dysfunction and constipation.

Through our systems-level analysis, we identified that *A. muciniphila*, *Erysipelatoclostridium*, and a species of *Eubacterium* contribute to increased production of tryptophan. Additionally, we found that serum levels of tryptophan betaine were significantly increased in patients with PD. We also found that serum levels of hippuric acid significantly increased in patients with PD. Hippuric acid has previously been reported to be increased in a metabolic profile of sebum from the upper back of patients with PD, contributing to the distinctive odor of people with PD (Trivedi et al., 2019). Previous studies have linked hippuric acid and IPA to the gut microbiota metabolism (Wikoff et al., 2009; Zhang and Davies, 2016). The conjugation between glycine and benzoic acid might originate hippuric acid, a reaction that can occur in the liver, kidney, and intestine (Wikoff et al., 2009). Similarly, our personalized gut microbial community modeling showed an increased level of glycine in patients with PD; therefore, gut microbial dysbiosis and changes in metabolite production levels in PD could contribute to the increased level of hippuric acid.

## STAR★METHODS

Detailed methods are provided in the online version of this paper and include the following:

- KEY RESOURCES TABLE
- RESOURCE AVAILABILITY
  - Lead contact
  - Materials availability
  - Data and code availability
- EXPERIMENTAL MODEL AND SUBJECT DETAILS
  - Human subjects
- METHOD DETAILS
  - Processing and downstream analysis of PD metagenomics
  - Richness and enterotype assessment
  - Identification of microbial compositional changes in PD dysbiosis, severity, gastrointestinal function and age
  - Carbohydrate-active enZymes annotation
  - Reconstruction of individual gut-microbial metabolic models of interest in PD dysbiosis, severity, gastrointestinal function and age
  - KEGG metabolic pathway analysis based on reactions abundance
  - Individual modeling simulations
  - Personalised gut-microbial-community metabolic models
  - Targeted metabolomics of serum samples from PD cohort
- QUANTIFICATION AND STATISTICAL ANALYSIS

## SUPPLEMENTAL INFORMATION

Supplemental Information can be found online at https://doi.org/10.1016/j.celrep.2021.108807.

## ACKNOWLEDGMENTS

This study was supported by Engineering and Physical Sciences Research Council (EPSRC) (EP/S001301/1), Biotechnology Biological Sciences Research Council (BBSRC) (BB/S016899/1), and Science for Life Laboratory. F.H.'s salary is funded by the BBSrC Institute Strategic Programme Gut Microbes and Health BB/r012490/1 and its constituent project BBS/e/F/000Pr10355. We are thankful to the entire staff of the Translational Systems Biology, Centre for Host-Microbiome Interactions, the Science for Life Laboratory, and Metagenopolis. The authors acknowledge the Swedish National Infrastructure for Computing at SNIC through Uppsala Multidisciplinary Center for Advanced Computational Science (UPPMAX) under projects SNIC 2019/3-226 and SNIC 2020/5-222. The authors also acknowledge King's College London computational infrastructure facility, Rosalind (https://rosalind.kcl.ac.uk), for high-performance computing. J.B. received honoraria for scientific presentations and travel grants from IPSEN Pharma Germany and Merz Pharmaceuticals Germany and is supported by the ParkinsonFonds Deutschland gGmbH and the Hilde Ulrich Stiftung for Parkinson's Research, Germany.

## AUTHOR CONTRIBUTIONS

S.S. and A.M. conceived and supervised the study. D.R., S.L., and E.L.C. performed the microbiome analysis. D.R. performed the integration of multi-omics data and modeling. G.B. reconstructed and refined the individual and community GEMs. J.B., F.H., and U.W. assisted in serum metabolomics and clinical metadata analysis. D.R. wrote the manuscript. S.S., S.D.E., M.U., and U.W. provided critical comments and feedback. All authors have revised and contributed to the final version.

## DECLARATION OF INTERESTS

The authors declare no competing interests.

Received: March 31, 2020
Revised: December 22, 2020
Accepted: February 9, 2021
Published: March 2, 2021

## REFERENCES

Aarsland, D., Creese, B., Politis, M., Chaudhuri, K.R., Ffytche, D.H., Weintraub, D., and Ballard, C. (2017). Cognitive decline in Parkinson disease. Nat. Rev. Neurol. *13*, 217–231.

Antony, P.M., Diederich, N.J., Krüger, R., and Balling, R. (2013). The hallmarks of Parkinson's disease. FEBS J. *280*, 5981–5993.

Arkin, A.P., Cottingham, R.W., Henry, C.S., Harris, N.L., Stevens, R.L., Maslov, S., Dehal, P., Ware, D., Perez, F., Canon, S., et al. (2018). KBase: The United States Department of Energy Systems Biology Knowledgebase. Nat. Biotechnol. *36*, 566–569.

Baldini, F., Heinken, A., Heirendt, L., Magnusdottir, S., Fleming, R.M.T., and Thiele, I. (2019). The Microbiome Modeling Toolbox: from microbial interactions to personalized microbial communities. Bioinformatics *35*, 2332–2334.

Baroncelli, R., Amby, D.B., Zapparata, A., Sarrocco, S., Vannacci, G., Le Floch, G., Harrison, R.J., Holub, E., Sukno, S.A., Sreenivasaprasad, S., and Thon, M.R. (2016). Gene family expansions and contractions are associated with host range in plant pathogens of the genus Colletotrichum. BMC Genomics *17*, 555.

Bedarf, J.R., Hildebrand, F., Coelho, L.P., Sunagawa, S., Bahram, M., Goeser, F., Bork, P., and Wüllner, U. (2017). Functional implications of microbial and viral gut metagenome changes in early stage L-DOPA-naïve Parkinson's disease patients. Genome Med. *9*, 39.

Benjamini, Y. (2010). Discovering the false discovery rate. J. R. Stat. Soc. Ser. A Stat. Soc. *71*, 405–416.

Bidkhori, G., Lee, S., Edwards, L.A., Le Chatelier, E., Almeida, M., Ezzamouri, B., Plaza Onate, F., Ponte, N., Shawcross, D.L., Proctor, G., et al. (2021). The Reactobiome Unravels a New Paradigm in Human Gut Microbiome Metabolism. bioRxiv. https://doi.org/10.1101/2021.02.01.428114.

Bolger, A.M., Lohse, M., and Usadel, B. (2014). Trimmomatic: a flexible trimmer for Illumina sequence data. Bioinformatics *30*, 2114–2120.

Borin, G.P., Sanchez, C.C., de Souza, A.P., de Santana, E.S., de Souza, A.T., Paes Leme, A.F., Squina, F.M., Buckeridge, M., Goldman, G.H., and Oliveira, J.V. (2015). Comparative Secretome Analysis of Trichoderma reesei and Aspergillus niger during Growth on Sugarcane Biomass. PLoS ONE *10*, e0129275.

Borre, Y.E., O'Keeffe, G.W., Clarke, G., Stanton, C., Dinan, T.G., and Cryan, J.F. (2014). Microbiota and neurodevelopmental windows: implications for brain disorders. Trends Mol. Med. *20*, 509–518.

Braak, H., de Vos, R.A., Bohl, J., and Del Tredici, K. (2006). Gastric alpha-synuclein immunoreactive inclusions in Meissner's and Auerbach's plexuses in cases staged for Parkinson's disease-related brain pathology. Neurosci. Lett. *396*, 67–72.

Breier, M., Wahl, S., Prehn, C., Fugmann, M., Ferrari, U., Weise, M., Banning, F., Seissler, J., Grallert, H., Adamski, J., and Lechner, A. (2014). Targeted metabolomics identifies reliable and stable metabolites in human serum and plasma samples. PLoS ONE *9*, e89728.

Brown, R.C., Lockwood, A.H., and Sonawane, B.R. (2005). Neurodegenerative diseases: an overview of environmental risk factors. Environ. Health Perspect. *113*, 1250–1256.

Cattaneo, A., Cattane, N., Galluzzi, S., Provasi, S., Lopizzo, N., Festari, C., Ferrari, C., Guerra, U.P., Paghera, B., Muscio, C., et al.; INDIA-FBP Group (2017). Association of brain amyloidosis with pro-inflammatory gut bacterial taxa and peripheral inflammation markers in cognitively impaired elderly. Neurobiol. Aging *49*, 60–68.

Chambers, J.C., McGregor, A., Jean-Marie, J., and Kooner, J.S. (1998). Acute hyperhomocysteinaemia and endothelial dysfunction. Lancet *351*, 36–37.

Chen, H., Zhang, S.M., Schwarzschild, M.A., Hernán, M.A., Logroscino, G., Willett, W.C., and Ascherio, A. (2004). Folate intake and risk of Parkinson's disease. Am. J. Epidemiol. *160*, 368–375.

Chen, S.G., Stribinskis, V., Rane, M.J., Demuth, D.R., Gozal, E., Roberts, A.M., Jagadapillai, R., Liu, R., Choe, K., Shivakumar, B., et al. (2016). Exposure to the Functional Bacterial Amyloid Protein Curli Enhances Alpha-Synuclein Aggregation in Aged Fischer 344 Rats and Caenorhabditis elegans. Sci. Rep. *6*, 34477.

Chiang, H.L., and Lin, C.H. (2019). Altered Gut Microbiome and Intestinal Pathology in Parkinson's Disease. J. Mov. Disord. *12*, 67–83.

Chin, J.H., and Vora, N. (2014). The global burden of neurologic diseases. Neurology *83*, 349–351.

Delday, M., Mulder, I., Logan, E.T., and Grant, G. (2019). Bacteroides thetaiotaomicron Ameliorates Colon Inflammation in Preclinical Models of Crohn's Disease. Inflamm. Bowel Dis. *25*, 85–96.

dos Santos, E.F., Busanello, E.N., Miglioranza, A., Zanatta, A., Barchak, A.G., Vargas, C.R., Saute, J., Rosa, C., Carrion, M.J., Camargo, D., et al. (2009). Evidence that folic acid deficiency is a major determinant of hyperhomocysteinemia in Parkinson's disease. Metab. Brain Dis. *24*, 257–269.

Duan, W., Ladenheim, B., Cutler, R.G., Kruman, I.I., Cadet, J.L., and Mattson, M.P. (2002). Dietary folate deficiency and elevated homocysteine levels endanger dopaminergic neurons in models of Parkinson's disease. J. Neurochem. *80*, 101–110.

Fasano, A., Visanji, N.P., Liu, L.W., Lang, A.E., and Pfeiffer, R.F. (2015). Gastrointestinal dysfunction in Parkinson's disease. Lancet Neurol. *14*, 625–639.

Forsyth, C.B., Shannon, K.M., Kordower, J.H., Voigt, R.M., Shaikh, M., Jaglin, J.A., Estes, J.D., Dodiya, H.B., and Keshavarzian, A. (2011). Increased intestinal permeability correlates with sigmoid mucosa alpha-synuclein staining and endotoxin exposure markers in early Parkinson's disease. PLoS ONE *6*, e28032.

Gaci, N., Borrel, G., Tottey, W., O'Toole, P.W., and Brugère, J.F. (2014). Archaea and the human gut: new beginning of an old story. World J. Gastroenterol. *20*, 16062–16078.

Gammon, K. (2014). Neurodegenerative disease: brain windfall. Nature *515*, 299–300.

Geisler-Lee, J., Geisler, M., Coutinho, P.M., Segerman, B., Nishikubo, N., Takahashi, J., Aspeborg, H., Djerbi, S., Master, E., Andersson-Gunneråas, S., et al. (2006). Poplar carbohydrate-active enzymes. Gene identification and expression analyses. Plant Physiol. *140*, 946–962.

Gerhardt, S., and Mohajeri, M.H. (2018). Changes of Colonic Bacterial Composition in Parkinson's Disease and Other Neurodegenerative Diseases. Nutrients *10*, 708.

Gu, C., Kim, G.B., Kim, W.J., Kim, H.U., and Lee, S.Y. (2019). Current status and applications of genome-scale metabolic models. Genome Biol. *20*, 121.

Guthikonda, S., and Haynes, W.G. (2006). Homocysteine: role and implications in atherosclerosis. Curr. Atheroscler. Rep. *8*, 100–106.

Holmes, I., Harris, K., and Quince, C. (2012). Dirichlet multinomial mixtures: generative models for microbial metagenomics. PLoS ONE *7*, e30126.

Horz, H.P., and Conrads, G. (2010). The discussion goes on: What is the role of Euryarchaeota in humans? Archaea *2010*, 967271.

Kanehisa, M., Furumichi, M., Tanabe, M., Sato, Y., and Morishima, K. (2017). KEGG: new perspectives on genomes, pathways, diseases and drugs. Nucleic Acids Res. *45*, D353–D361.

Keshavarzian, A., Green, S.J., Engen, P.A., Voigt, R.M., Naqib, A., Forsyth, C.B., Mutlu, E., and Shannon, K.M. (2015). Colonic bacterial composition in Parkinson's disease. Mov. Disord. *30*, 1351–1360.

Kim, S., Kwon, S.H., Kam, T.I., Panicker, N., Karuppagounder, S.S., Lee, S., Lee, J.H., Kim, W.R., Kook, M., Foss, C.A., et al. (2019). Transneuronal Propagation of Pathologic α-Synuclein from the Gut to the Brain Models Parkinson's Disease. Neuron *103*, 627–641.e7.

Kovatcheva-Datchary, P., Shoaie, S., Lee, S., Wahlström, A., Nookaew, I., Hallen, A., Perkins, R., Nielsen, J., and Bäckhed, F. (2019). Simplified Intestinal Microbiota to Study Microbe-Diet-Host Interactions in a Mouse Model. Cell Rep. *26*, 3772–3783.e6.

Langmead, B., and Salzberg, S.L. (2012). Fast gapped-read alignment with Bowtie 2. Nat. Methods *9*, 357–359.

Le Chatelier, E., Nielsen, T., Qin, J., Prifti, E., Hildebrand, F., Falony, G., Almeida, M., Arumugam, M., Batto, J.M., Kennedy, S., et al.; MetaHIT

Consortium (2013). Richness of human gut microbiome correlates with metabolic markers. Nature *500*, 541–546.

Lee, H.M., and Koh, S.B. (2015). Many Faces of Parkinson's Disease: Non-Motor Symptoms of Parkinson's Disease. J. Mov. Disord. *8*, 92–97.

Ma, M.J. (2018). Biopsy Pathology of Neurodegenerative Disorders in Adults. In Practical Surgical Neuropathology: A Diagnostic Approach, Second Edition, A. Perry and D.J. Brat, eds. (Elsevier), pp. 659–680.

Mardinoglu, A., Shoaie, S., Bergentall, M., Ghaffari, P., Zhang, C., Larsson, E., Bäckhed, F., and Nielsen, J. (2015). The gut microbiota modulates host amino acid and glutathione metabolism in mice. Mol. Syst. Biol. *11*, 834.

Mardinoglu, A., Boren, J., Smith, U., Uhlen, M., and Nielsen, J. (2018). Systems biology in hepatology: approaches and applications. Nat. Rev. Gastroenterol. Hepatol. *15*, 365–377.

Müller, T. (2008). Role of homocysteine in the treatment of Parkinson's disease. Expert Rev. Neurother. *8*, 957–967.

Müller, T., and Kuhn, W. (2009). Homocysteine levels after acute levodopa intake in patients with Parkinson's disease. Mov. Disord. *24*, 1339–1343.

Pfeiffer, R.F. (2011). Gastrointestinal dysfunction in Parkinson's disease. Parkinsonism Relat. Disord. *17*, 10–15.

Rohart, F., Gautier, B., Singh, A., and Lê Cao, K.A. (2017). mixOmics: An R package for 'omics feature selection and multiple data integration. PLoS Comput. Biol. *13*, e1005752.

Rosario, D., Benfeitas, R., Bidkhori, G., Zhang, C., Uhlen, M., Shoaie, S., and Mardinoglu, A. (2018). Understanding the Representative Gut Microbiota Dysbiosis in Metformin-Treated Type 2 Diabetes Patients Using Genome-Scale Metabolic Modeling. Front. Physiol. *9*, 775.

Rosario, D., Boren, J., Uhlen, M., Proctor, G., Aarsland, D., Mardinoglu, A., and Shoaie, S. (2020). Systems Biology Approaches to Understand the Host-Microbiome Interactions in Neurodegenerative Diseases. Front. Neurosci. *14*, 716.

Sampson, T.R., Debelius, J.W., Thron, T., Janssen, S., Shastri, G.G., Ilhan, Z.E., Challis, C., Schretter, C.E., Rocha, S., Gradinaru, V., et al. (2016). Gut Microbiota Regulate Motor Deficits and Neuroinflammation in a Model of Parkinson's Disease. Cell *167*, 1469–1480.e12.

Sampson, T.R., Challis, C., Jain, N., Moiseyenko, A., Ladinsky, M.S., Shastri, G.G., Thron, T., Needham, B.D., Horvath, I., Debelius, J.W., et al. (2020). A gut bacterial amyloid promotes α-synuclein aggregation and motor impairment in mice. eLife *9*, e53111.

Savica, R., Carlin, J.M., Grossardt, B.R., Bower, J.H., Ahlskog, J.E., Maraganore, D.M., Bharucha, A.E., and Rocca, W.A. (2009). Medical records documentation of constipation preceding Parkinson disease: A case-control study. Neurology *73*, 1752–1758.

Schellenberger, J., Que, R., Fleming, R.M., Thiele, I., Orth, J.D., Feist, A.M., Zielinski, D.C., Bordbar, A., Lewis, N.E., Rahmanian, S., et al. (2011). Quantitative prediction of cellular metabolism with constraint-based models: the COBRA Toolbox v2.0. Nat. Protoc. *6*, 1290–1307.

Scheperjans, F., Aho, V., Pereira, P.A., Koskinen, K., Paulin, L., Pekkonen, E., Haapaniemi, E., Kaakkola, S., Eerola-Rautio, J., Pohja, M., et al. (2015). Gut microbiota are related to Parkinson's disease and clinical phenotype. Mov. Disord. *30*, 350–358.

Shannon, P., Markiel, A., Ozier, O., Baliga, N.S., Wang, J.T., Ramage, D., Amin, N., Schwikowski, B., and Ideker, T. (2003). Cytoscape: a software environment for integrated models of biomolecular interaction networks. Genome Res. *13*, 2498–2504.

Shoaie, S., Karlsson, F., Mardinoglu, A., Nookaew, I., Bordel, S., and Nielsen, J. (2013). Understanding the interactions between bacteria in the human gut through metabolic modeling. Sci. Rep. *3*, 2532.

Shoaie, S., Ghaffari, P., Kovatcheva-Datchary, P., Mardinoglu, A., Sen, P., Pujos-Guillot, E., de Wouters, T., Juste, C., Rizkalla, S., Chilloux, J., et al.; MICRO-Obes Consortium (2015). Quantifying Diet-Induced Metabolic Changes of the Human Gut Microbiome. Cell Metab. *22*, 320–331.

Tramontano, M., Andrejev, S., Pruteanu, M., Klünemann, M., Kuhn, M., Galardini, M., Jouhten, P., Zelezniak, A., Zeller, G., Bork, P., et al. (2018). Nutritional preferences of human gut bacteria reveal their metabolic idiosyncrasies. Nat. Microbiol. *3*, 514–522.

Triantafyllou, K., Chang, C., and Pimentel, M. (2014). Methanogens, methane and gastrointestinal motility. J. Neurogastroenterol. Motil. *20*, 31–40.

Trivedi, D.K., Sinclair, E., Xu, Y., Sarkar, D., Walton-Doyle, C., Liscio, C., Banks, P., Milne, J., Silverdale, M., Kunath, T., et al. (2019). Discovery of Volatile Biomarkers of Parkinson's Disease from Sebum. ACS Cent. Sci. *5*, 599–606.

Tuomainen, M., Lindström, J., Lehtonen, M., Auriola, S., Pihlajamäki, J., Peltonen, M., Tuomilehto, J., Uusitupa, M., de Mello, V.D., and Hanhineva, K. (2018). Associations of serum indolepropionic acid, a gut microbiota metabolite, with type 2 diabetes and low-grade inflammation in high-risk individuals. Nutr. Diabetes *8*, 35.

Wegmann, U., Louis, P., Goesmann, A., Henrissat, B., Duncan, S.H., and Flint, H.J. (2014). Complete genome of a new Firmicutes species belonging to the dominant human colonic microbiota ('Ruminococcus bicirculans') reveals two chromosomes and a selective capacity to utilize plant glucans. Environ. Microbiol. *16*, 2879–2890.

Wen, C., Zheng, Z., Shao, T., Liu, L., Xie, Z., Le Chatelier, E., He, Z., Zhong, W., Fan, Y., Zhang, L., et al. (2017). Quantitative metagenomics reveals unique gut microbiome biomarkers in ankylosing spondylitis. Genome Biol. *18*, 142.

Wikoff, W.R., Anfora, A.T., Liu, J., Schultz, P.G., Lesley, S.A., Peters, E.C., and Siuzdak, G. (2009). Metabolomics analysis reveals large effects of gut microflora on mammalian blood metabolites. Proc. Natl. Acad. Sci. USA *106*, 3698–3703.

Witherden, E.A., Moyes, D.L., Bruce, K.D., Ehrlich, S.D., and Shoaie, S. (2017). Using systems biology approaches to elucidate cause and effect in host–microbiome interactions. Curr. Opin. Syst. Biol. *3*, 141–146.

Wlodarska, M., Luo, C., Kolde, R., d'Hennezel, E., Annand, J.W., Heim, C.E., Krastel, P., Schmitt, E.K., Omar, A.S., Creasey, E.A., et al. (2017). Indoleacrylic Acid Produced by Commensal Peptostreptococcus Species Suppresses Inflammation. Cell Host Microbe *22*, 25–37.e6.

Wu, H., Esteve, E., Tremaroli, V., Khan, M.T., Caesar, R., Mannerås-Holm, L., Ståhlman, M., Olsson, L.M., Serino, M., Planas-Fèlix, M., et al. (2017). Metformin alters the gut microbiome of individuals with treatment-naive type 2 diabetes, contributing to the therapeutic effects of the drug. Nat. Med. *23*, 850–858.

Xie, Y., Feng, H., Peng, S., Xiao, J., and Zhang, J. (2017). Association of plasma homocysteine, vitamin B12 and folate levels with cognitive function in Parkinson's disease: A meta-analysis. Neurosci. Lett. *636*, 190–195.

Zhang, L.S., and Davies, S.S. (2016). Microbial metabolism of dietary components to bioactive metabolites: opportunities for new therapeutic interventions. Genome Med. *8*, 46.

Zhang, H., Yohe, T., Huang, L., Entwistle, S., Wu, P., Yang, Z., Busk, P.K., Xu, Y., and Yin, Y. (2018). dbCAN2: a meta server for automated carbohydrate-active enzyme annotation. Nucleic Acids Res. *46* (*W1*), W95–W101.

Zhao, Z.H., Xin, F.Z., Xue, Y., Hu, Z., Han, Y., Ma, F., Zhou, D., Liu, X.L., Cui, A., Liu, Z., et al. (2019). Indole-3-propionic acid inhibits gut dysbiosis and endotoxin leakage to attenuate steatohepatitis in rats. Exp. Mol. Med. *51*, 1–14.

## STAR★METHODS

### KEY RESOURCES TABLE

| SOFTWARE and ALGORITHMS | SOURCE | IDENTIFIER |
|---|---|---|
| Meteor | (N. Pons et al., 2010, JOBIM, conference; Wen et al., 2017) | https://www.academia.edu/14061278/METEOR_a_plateform_for_quantitative_metagenomic_profiling_of_complex_ecosystems |
| Trimmomatic | Bolger et al., 2014 | http://www.usadellab.org/cms/?page=trimmomatic |
| Bowtie2 | Langmead and Salzberg, 2012 | http://bowtie-bio.sourceforge.net/bowtie2/index.shtml |
| Integrated Gut Catalog version 2 (IGC2) | Wen et al., 2017 | https://data.inrae.fr/dataset.xhtml?persistentId=doi:10.15454/QVCYRB |
| MetaOMineR | Le Chatelier et al., 2013 | https://cran.r-project.org/web/packages/momr/index.html |
| KEGG | Kanehisa et al., 2017 | https://www.genome.jp/kegg/ |
| dbCAN2 | Zhang et al., 2018 | http://bcb.unl.edu/dbCAN2/index.php |
| Cytoscape | Shannon et al., 2003 | https://cytoscape.orgversion3.7.1 |
| DirichletMultinomial | Holmes et al., 2012 | http://bioconductor.org/packages/release/bioc/html/DirichletMultinomial.html |
| KBase | Arkin et al., 2018 | https://www.kbase.us |
| COnstraint-Based Reconstruction and Analysis (COBRA) Toolbox (v2.0) | Schellenberger et al., 2011 | https://opencobra.github.io/cobratoolbox/stable/index.html |
| mixOmics package | Rohart et al., 2017 | https://www.bioconductor.org/packages/release/bioc/html/mixOmics.html |
| MIGRENE Toolbox | Bidkhori et al., 2021 | https://github.com/sysbiomelab/MIGRENE |

### RESOURCE AVAILABILITY

#### Lead contact

Further information and requests for resources and reagents should be directed to and will be fulfilled by Saeed Shoaie (saeed.shoaie@kcl.ac.uk).

#### Materials availability

This study did not generate new reagents.

#### Data and code availability

The metagenomics sequences were downloaded from the original study repository deposited in the European Bioinformatics Institute-Sequence Read Archive database, under accession number ERP019674. The metabolomics data can be found in the Table S3.

### EXPERIMENTAL MODEL AND SUBJECT DETAILS

#### Human subjects

We downloaded publicly available shotgun metagenomics data from a German PD cohort (Bedarf et al., 2017) consisted of 31 early stage, L-DOPA-naive patients with PD and 28 age and male-sex matched controls from European Nucleotide Archive (ENA) repository, ID ERP019674, project description: faecal microbiota in a L-DOPA naive PD patient. We removed some of the samples and re-analyzed the metagenomics data of 26 PD and 25 controls, of which 11 were healthy controls (CO) while 14 were diseased controls with cardiovascular risk factors (DC). Clinical characteristics of the individual's cohort are detailed in Table S4.

Serum samples from 8 people with PD, 5 CO and 5 DC of the same cohort were obtained via peripheral venous sampling following centrifugation (10 min. at 2.000 g at 20°C). The study was approved by the local ethics committee of the University of Bonn. The participants in the study were recruited from the Department of Neurology at the University of Bonn and all gave informed consent (internal ethics vote 126/02). Supernatants were stored at −80°C prior to analysis.

## METHOD DETAILS

### Processing and downstream analysis of PD metagenomics

We downloaded publicly available shotgun metagenomics data from a German PD cohort (Bedarf et al., 2017) consisted of 31 early stage, L-DOPA-naive patients with PD and 28 age and male-sex matched controls from European Nucleotide Archive (ENA) repository, ID ERP019674, project description: faecal microbiota in a L-DOPA naive PD patient. The metagenomics cohort have been composed by Illumina HiSeq 2500 paired end sequencing runs belonging to patients with PD and controls, where these were sub-grouped into healthy controls and disease controls with cardiovascular risk factors. We used Meteor (Bolger et al., 2014; Langmead and Salzberg, 2012; N. Pons et al., 2010, JOBIM, conference; Wen et al., 2017), a software for quantitative metagenomic profiling of complex ecosystems, to generate the gene abundance profiling table. First, only reads mapping to an unique gene part of the gut catalog were attributed to those corresponding genes. Second, reads mapping to multiple genes existent in the catalog were attributed considering the ratio of the unique mapping counts of the genes. MetaOMineR (Le Chatelier et al., 2013) was applied for gene counts table normalization process and further downstream analysis.

We observed that downstream analysis of metagenomics data is strongly affected by variability in sequencing depth. Therefore, we downsized the data before normalizing the gene counts to reduce this effect, as this may bias our downstream analysis. This process requires compromising the loss of information with the gain of identified MSPs. A level of minimum 10 million reads was defined as threshold for downsizing with 1 repetition, previous to normalization of the raw gene counts table. Such process requires a compromise between loss of information (data, here samples) and later gain of identified MSPs, which is defined by the downsizing threshold. We removed some of the samples and re-analyzed the metagenomics data of 26 PD and 25 controls, of which 11 were healthy controls (CO) while 14 were diseased controls with cardiovascular risk factors (DC). Samples metadata, namely, age, UPDRSIII score and GSRS score can be found in Table S4.

### Richness and enterotype assessment

Gene richness is highly sensitive to sequencing depth, therefore, level of downsizing applied was of 10 million reads, with 30 repetitions, from which the mean was considered as the richness. To assess samples' bacterial diversity gene richness was obtained based on the downsized and normalized gene counts table, while MSP richness based on clustered MSPs table. DirichletMultinomial (Holmes et al., 2012) for Clustering and Classification of Microbiome Data was applied to identify samples enterotype, by defining three Dirichlet components to model and by providing genera count data.

### Identification of microbial compositional changes in PD dysbiosis, severity, gastrointestinal function and age

Significant taxonomic alterations between PD and were determined by Wilcoxon signed-rank test and by correcting the *P values* for multiple testing applying Benjamini-Hochberg false discovery rate (FDR) (Benjamini, 2010), q-values. PD samples were grouped into quartiles considering metadata, namely: (1) UPDRSIII scores, here denoted as PD severity; (2) a modified version of GSRS scores (see original study) resembling GI function across people with PD; (3) age. Significant taxonomic alterations between $1^{st}$ and $4^{th}$ quartiles of each metadata variable were obtained as previously mentioned for PD against controls. Spearman correlation between PD metadata and MSPs abundances was determined and adjusted for FDR. Cytoscape (Shannon et al., 2003) was used to construct an integrative correlation network (ICN) between PD dysbiosis against controls, PD clinical parameters under study and respective significant and/or correlated MSPs abundances. ICN enabled us to identified known species commonly altered in different clinical parameters of PD, as well as perturbed MSPs uniquely related to one of these clinical parameters. Based on this representation, we can identify known species and if its alteration in abundance is related to more than one clinical parameter in PD and which type of associations exists.

### Carbohydrate-active enZymes annotation

Gut catalog genes (Wen et al., 2017) respective to MSPs found significantly altered considering PD dysbiosis (PD against controls), severity (UPDRSIII score), GI function (GSRS score) and age were annotated to dbCAN2 (Zhang et al., 2018). Subsequently, identification of substrate conversion from annotated Carbohydrate-Active enZymes (CAZymes) was performed based on literature review (Baroncelli et al., 2016; Borin et al., 2015; Breier et al., 2014; Geisler-Lee et al., 2006; Wegmann et al., 2014).

### Reconstruction of individual gut-microbial metabolic models of interest in PD dysbiosis, severity, gastrointestinal function and age

GEMs reconstruction was performed based on genes from the gut catalog binned into MSPs. KEGG Ontology (KO) (Kanehisa et al., 2017) annotation for IGC2 genes was mapped to reference model reactions from KBase (Arkin et al., 2018). Reaction score was obtained based on the catalog for each microbe. Biomass and exchange reactions were functionally defined together with gap filling using COnstraint-Based Reconstruction and Analysis (COBRA) Toolbox (Schellenberger et al., 2011) and the KBase originated reference model. The simulation of functional GEMs was then constrained based on western diet in anaerobic conditions.

### KEGG metabolic pathway analysis based on reactions abundance

The Microbial and personalized GEM, REactobiome and community NEtwork modeling (MIGRENE) toolbox (https://github.com/sysbiomelab/MIGRENE) (Bidkhori et al., 2021) was used for reaction abundance and enrichment analysis. KEGG metabolic pathways prevalence and maximal coverage was determined based on pathway presence and respective coverage in the generated microbial GEMs. Equally sized sets of top most significantly increased and decreased MSPs for each PD condition under study were defined, namely: 46 most significantly increased and 46 most significantly decreased between PD and controls (dysbiosis), top ten for severity, top nine for GI function and top 14 for age. A threshold of at least 15% was used to identify differently prevalent metabolic pathways, as well as the maximal pathway coverage found in each set of MSPs. Microbial reaction abundance per sample of the PD metagenomics cohort was determined based on each MSP identified per sample that we could originate a functional metabolic model. A reaction pool was generated, and reactions were multiplied by MSP abundance in each sample. Personalised reaction abundance was calculated based on the summation of each reaction frequency within each individual-microbiota. Reactions with significantly different abundances were identified by Wilcoxon signed-rank test ($p$ value $< 0.05$) for PD dysbiosis, severity, GI dysfunction and age. Significant reactions were mapped to respective KOs, or Enzyme Commission number (EC number) when KO was not available, which in turn were mapped to KEGG metabolic pathways. The metabolic pathway enrichment was performed based on microbial reaction presence retrieved from the metabolic models in each PD cohort sample. Hypergeometric test was applied for pathway enrichment. Significant ($p$ value $< 0.05$) enriched pathways were identified using Wilcoxon signed-rank test.

### Individual modeling simulations

COBRA Toolbox was used to define simulations settings. Predictions given specified parameters (e.g., diet constrains under anaerobic conditions) were performed based on flux balance analysis (FBA) with biomass defined as cellular objective. Microbial growth rate and metabolites consumption and production by microbes was determined by FBA. Functional individual metabolic model representative of each condition of interest (PD dysbiosis, severity, GI dysfunction and age) were selected based on equally sized sets of top most significantly increased and decreased MSPs, as previously applied in metabolic pathways prevalence.

### Personalised gut-microbial-community metabolic models

Personalised community models were reconstructed for each sample in the PD cohort, using MIGRENE toolbox (Bidkhori et al., 2021). Due to computational power requirements and in order to assure model functionality, a maximum of 50 MSPs per community was stablished. Microbial *S matrices* were combined guaranteeing that each microbe would have their own cellular compartment. Besides microbial cells, it was designed a compartment representative of the intestinal lumen where metabolites derived from food ingestion would be available. Additionally, another compartment was designed for secreted microbial-metabolites and remaining food-derived metabolites that were not consumed by bacteria. These represent microbial metabolites that can be absorbed and reach the human blood circulation or instead be found in human faeces. Community-microbial biomass function is composed by biomass functions of each microbe constituent of the community. For each community, each individual microbe biomass function was constrained based on respective abundance in that specific sample. Community biomass was defined as objective function. Each personalised community contains the top most abundant MSPs in each particular individual till it reaches 50 bacteria per community. For each community, we performed FBA with cellular objective defined as biomass and we collected the predicted fluxes of exchange reactions representing food-derived metabolites (FoEx) and microbial-derived metabolites (FeEx). The difference between FeEx and FoEx fluxes was determined. Significantly different FeEx production between PD and controls was identified based on Wilcoxon signed-rank test ($p$ value $< 0.05$).

Reactions of interest were defined as personalised community model objective to identify principal microbial producers. Models with similar number of productions across communities in both groups, namely PD and controls, were ignored, in order to identify main contributors to increased or decreased secretions in PD. Only microbial models with production in at least 3 communities in the group were considered. Correlation analysis between predicted metabolites fluxes from personalized community modeling and MSPs abundances from metagenomics samples was performed. We have calculated the variation between in (FoEx) and out (FeEx) fluxes and correlated it with MSPs abundances. Significant ($p$ value $< 0.01$) spearman correlations were determined.

### Targeted metabolomics of serum samples from PD cohort

Serum samples from 8 PD samples, 5 CO and 5 DC were obtained via peripheral venous sampling following centrifugation (10 min. at 2.000 g at 20°C). The study was approved by the local ethics committee of the University of Bonn. The participants in the study were recruited from the Department of Neurology at the University of Bonn and all gave informed consent (internal ethics vote 126/02). Supernatants were stored at −80°C prior to analysis. Targeted (mass spectrometry-based) metabolomics was generated by Biocrates' MxP® Quant 500 kit (Table S3). The kit allows the quantification of endogenous metabolites from diverse biochemical classes. Case and control average of each analyte absolute concentration (μM) was clustered into and represented by analyte class. For a matter of representation, analyte relative concentrations were determined. Partial Least-squares-Discriminant Analysis (PLS-DA) was performed using mixOmics (Rohart et al., 2017) package. PLS-DA was performed between PD and control groups separately. Significant alterations of metabolite concentration between PD and controls were determined by Wilcoxon signed-rank test ($p$ value $< 0.05$). Spearman correlation was determined between metabolites concentration and MSPs abundances.

## QUANTIFICATION AND STATISTICAL ANALYSIS

Statistical analysis was performed using R software v 3.6.1. Significant taxonomic alterations between PD and were determined by Wilcoxon signed-rank test and by correcting the *P value*s for multiple testing applying Benjamini-Hochberg false discovery rate (FDR) (Benjamini, 2010), q-values (significance FDR < 0.05), which can be found in Figure 1. Reactions with significantly different abundances were identified by Wilcoxon signed-rank test (p value < 0.05) for PD dysbiosis, severity, GI dysfunction and age, in Figure 2. Significant (p value < 0.05) enriched pathways were identified using Wilcoxon signed-rank test, in Figure 2. The difference between FeEx and FoEx fluxes was determined. Significantly different FeEx production between PD and controls was identified based on Wilcoxon signed-rank test (p value < 0.05). We have calculated the variation between in (FoEx) and out (FeEx) fluxes and correlated it with MSPs abundances. Significant (p value < 0.01) spearman correlations were determined, found in Table S5. Significant alterations of metabolite concentration between PD and controls were determined by Wilcoxon signed-rank test (p value < 0.05), represented in Figure 4.